

Development of the Torso Robot – Design of the New Shoulder Mechanism ‘Cybernetic Shoulder’

Yoshihiko NAKAMURA Masafumi OKADA Shin-ichirou HOSHINO
University of Tokyo, Department of Mechano-Informatics
7-3-1 Hongo Bunkyo-ku Tokyo 113, Japan
nakamura, okada, hoshino@ynl.t.u-tokyo.ac.jp

Abstract: In this paper, we develop a three DOF mechanism for humanoid robots, which we call the cybernetic shoulder. This mechanism imitates the motion of the human shoulder and does not have a fixed center of rotation, which enables unique human-like motion in contrast to the conventional design of anthropomorphic seven DOF manipulators that have base three joint axes intersecting at a fixed point. Taking advantage of the cybernetic shoulder's closed-link structure, we can easily introduce the programmable passive compliance adopting the actuation redundancy and elastic members. This is important for the integrated safety of humanoid robots that are inherently required to physically interact with the human.

1. Introduction

The humanoid robot is similar to a human, has same degree-of-freedom as a human, and can do same works as a human. Many researches have been made for it [1]~[4]. The most important demands for humanoid robots are as follows:

1. **Human-Like Mobility** To have human-like geometry would be a requirement for a humanoid robot working among the humans since it provides with a geometric sufficiency for the robot working in the structured environment by the humans. The same reasoning applies to the mobility of humanoid robots. Moving, namely reaching and walking, like the humans is important from the geometric functionality point of view as well as the psychological point of view.
2. **Human-Like Compliance** Working and moving among humans requires special concerns on the safety issues. A humanoid robot should weigh not significantly more than a human. Mechanical compliance of the surfaces and joints is also a necessity.

In this paper, we propose a new shoulder mechanism for humanoid robots. A closed kinematic chain with three degree-of-freedom structured mechanism, which meets the first requirement and potentially enables the implementation of the second requirement. We call this mechanism the cybernetic shoulder.

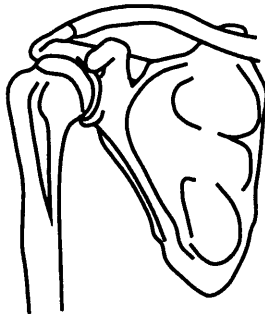


Figure 1. Human shoulder mechanism

2. Human Shoulder Mechanism

Figure 1 shows the human shoulder mechanism. The human shoulder is composed by 5 joints so that it can move smoothly, which is caused by a collarbone[5]. Figure 2 shows the motion of the human shoulder. This figure means that the human shoulder's motion does not have a fixed center of rotation. We consider that causes the human-like motion. The conventional design

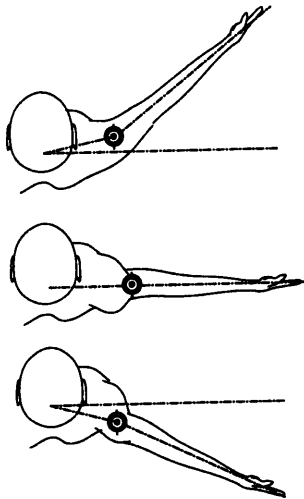


Figure 2. Motion of the human shoulder

of anthropomorphic seven degree-of-freedom manipulators cannot realize this motion.

3. Cybernetic Shoulder

3.1. A Mechanism of the Cybernetic Shoulder

Figure 3 shows the model of the cybernetic shoulder. This mechanism imitates the human shoulder geometry and has a human-like motion. β and δ are two degree-of-freedom gimbal mechanisms, d is a ball joint, b is a two degree-of-

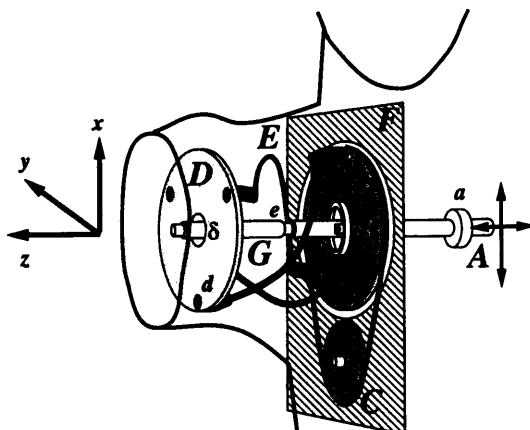


Figure 3. Cybernetic shoulder

freedom universal joint, a is a four degree-of-freedom spherical and prismatic joint and e is a prismatic joint. Moving point A within vertical plane alters the pointing direction of the main shaft G , which determines, along with the constraints due to the free curved links E between points b and d , the direction of the normal vector of D . The rotation about the normal of D is mainly determined by the rotation of C through B and E . Note that the rotation of C affects the pointing direction of D when B and D are no longer parallel. The advantages of this mechanism are summarized as follows.

Compactness Since the cybernetic shoulder can locate its actuators inside the chest, the shoulder geometry occupies rather small volume and shows a smooth shape, compared with the conventional designs of shoulder joints of manipulators.

Large mobile area In this mechanism, the angle magnification ratio can be wide, which causes the large mobile area. Figure 4 shows the motion of the cybernetic shoulder, as of the reduced two dimensional model. When the link G rotates ψ within ± 45 degree, the normal vector of D rotates within ± 90 degree.

Human like motion As we mentioned, this mechanism imitates the human shoulder motion and does not have a fixed center of rotation. Figure 5 shows a locus of centers of rotation when it moves along y axis.

From these figures we can understand that the cybernetic shoulder does not have a fixed center of rotation, which is same as human shoulder motion shown in Fig.2. It is impossible for conventional design of anthropomorphic three degree-of-freedom mechanisms.

Singularity Free In theory, link G can rotate within ± 90 degrees, namely ψ can rotate in the range of $|\psi| < 90$ degrees. When ψ equals to ± 90 degrees, point A should move an infinite distance even for a small required motion

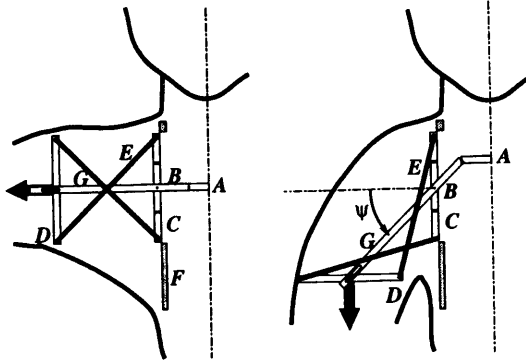


Figure 4. Motion of the Cybernetic Shoulder

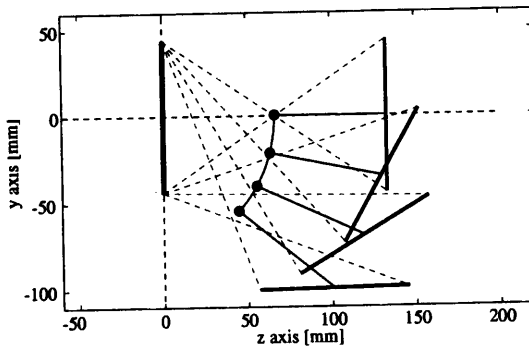


Figure 5. Center of rotation

of plate D , namely it is a singular point. In practice, mechanical design may limit the range of ψ a bit smaller. In the two dimensional model, ψ can rotate to 45 degrees, and the normal vector of plate D can rotate to 90 degrees. Although the upper limit of ψ depends on the rotation about the z axis in the three dimensional model, whose effect is not much. In our prototype, the range of ψ takes ± 45 degrees at the minimum. This range of ψ , along with the coupled change of the center of rotation of plate D , keeps the work space of arms larger than the conventional design. Note that there is no shoulder singularity within the workspace.

Small Backlash The cybernetic shoulder has a double universal-joint structure which yields a human shoulder geometry and has a human like motion[3]. Many types of double universal-joint structures were developed [3, 6, 7], where the double universal-joint mechanisms were driven by gears, and resulted in large backlash. On the other hand, the kinematic constraint of the cybernetic shoulder is provided by the closed kinematic chains, which realizes small backlash.

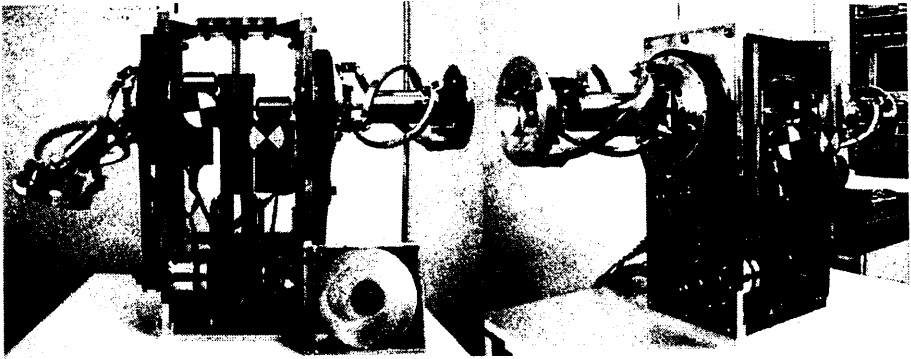


Figure 6. Photographs of the cybernetic shoulder

Figure 6 and 7 show photographs of a prototype of the cybernetic shoulder. The height of the body is about 400mm and the width between the end of the left shoulder and right shoulder is about 600mm. The diameter of D is about 110mm. Three actuators are DC motors of 90W. The planner motion of point A is made by two perpendicular ball-screw axes assembled in series.

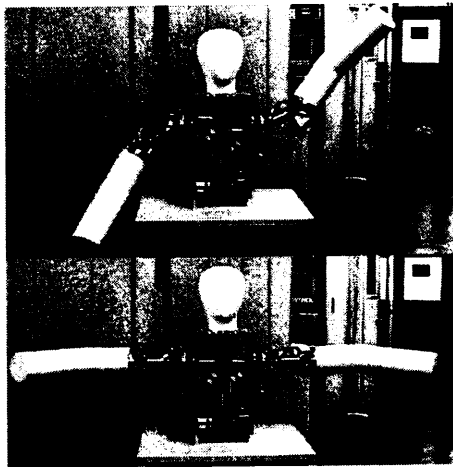


Figure 7. Motion of the experimental system

3.2. Kinematics of the cybernetic shoulder

Due to the complexity of a closed kinematic chain, it is difficult to get a closed form solution of the inverse or the forward kinematics. Therefore we develop a numerical method to solve the kinematics.

We define parameters and coordinate systems as shown in Fig.8. $x_0y_0z_0$ is the absolute coordinate system which has the origin at the β , center of B . $x_1y_1z_1$ is the end plate coordinate system which has the origin at the δ , center

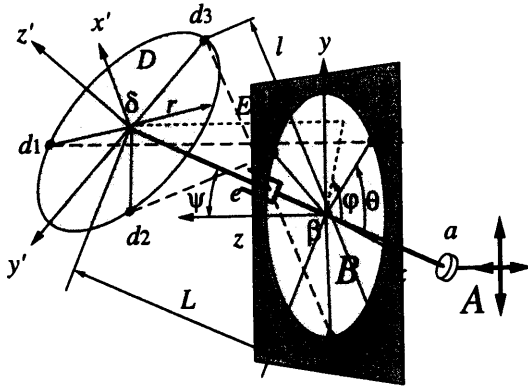


Figure 8. Model of the cybernetic shoulder

of D . In the initial condition, b_1 has the same direction as x_0 . In Fig.8, $x_0 y_0 z_0$ is rotated ϕ around the z_0 axis. In the following, $[\cdot]^i$ means a vector in the $x_i y_i z_i$ coordinate system and R_θ^ξ implies the rotation θ around the ξ axis. Accordingly Fig.8

$$b_i^0 = R_\phi^{z_0} R_{\frac{2}{3}(i-1)\pi}^{z_0} [r \ 0 \ 0]^T \tag{1}$$

$$d_i^1 = R_{\frac{2}{3}(i-1)\pi}^{z_0} [r \ 0 \ 0]^T \tag{2}$$

are satisfied. Since β and δ have a gimbal mechanism, we can consider a θ_{x_0} rotation about the x_0 axis, a θ_{y_0} rotation about the y_0 axis, a θ_{x_1} rotation about the x_1 axis and a θ_{y_1} rotation about the y_1 axis. We now obtain the following equations:

$$d_i^0 = \delta + R d_i^1 \quad (i = 1, 2, 3) \tag{3}$$

$$\delta := L R_A e_z \tag{4}$$

$$R := R_A R_B \tag{5}$$

$$R_A := R_{\theta_{x_0}}^{x_0} R_{\theta_{y_0}}^{y_0} \tag{6}$$

$$R_B := R_{\theta_{y_1}}^{y_1} R_{\theta_{x_1}}^{x_1} \tag{7}$$

$$e_z = [0 \ 0 \ 1]^T \tag{8}$$

where $\theta_{x_0}, \theta_{y_0}$ and ϕ are given by the position of A and the rotation angle of C . Any parameters such as $\theta_{x_1}, \theta_{y_1}$ and L are unknown. The kinematic constraints of the mechanism are represented by that the lengths of link E are constant. Namely,

$$|d_i^0 - b_i^0|^2 = \ell^2 \tag{9}$$

From equation (3), (9) is written as follows:

$$|L R_A e_z + R d_i^1 - b_i^0|^2 = \ell_i^2 \tag{10}$$

which is then expanded in the following form:

$$2Le_z^T R_A^T (R_A R_B d_i^1 - b_i^0) - 2b_i^{0T} R_A R_B d_i^1 + L^2 + 2r^2 - \ell_i^2 = 0 \quad (i = 1, 2, 3) \quad (11)$$

We apply numerical computation to solve equation (11).

4. Design of the passive compliance

4.1. Design of a compliant link

A humanoid robot should have a mechanical softness so as not to injure the people sharing the space. Since the cybernetic shoulder is composed of a closed kinematic chain, we can design the softness of mechanism.

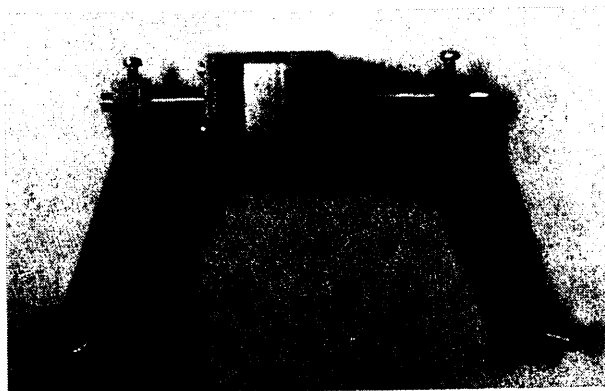


Figure 9. Compliant link with damper

Table 1. Spring constant of links

Material	Spring constant (N/m)
1. $\phi 3\text{mm}$ carbon fiber	1456.7
2. $\phi 5\text{mm}$ carbon fiber	5845.5
3. $\phi 4.31\text{mm}$ SMA	2295.5
4. Aluminum alloy	15775.0

Figure 9 shows the compliant link of a $\phi 5\text{mm}$ carbon fiber rod fiber and a damper, which is designed as seen in Figure 10. Assembled two thick squared rings in chain form three chambers, which are filled with Temper Foam^{®†}. By replacing this material with alternatives one, we can design the elasticity and viscosity of a link. We prototyped four types of elastic link. The configuration and the spring constant of these links are shown in Table 4.1. While the aluminum alloy link shows rather rigid property, links designed by using carbon fiber rod and a shape memory alloy possesses flexibility of different levels.

[†]Temper Foam : Produced by EAR SPECIALITY COMPOSITES Corp. shows frequency dependent characteristics. Namely, it shows high stiffness for high frequency, high viscosity for low frequency.

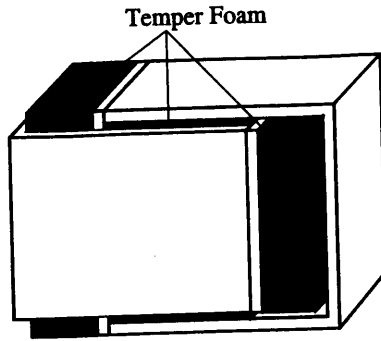


Figure 10. Design of a damper

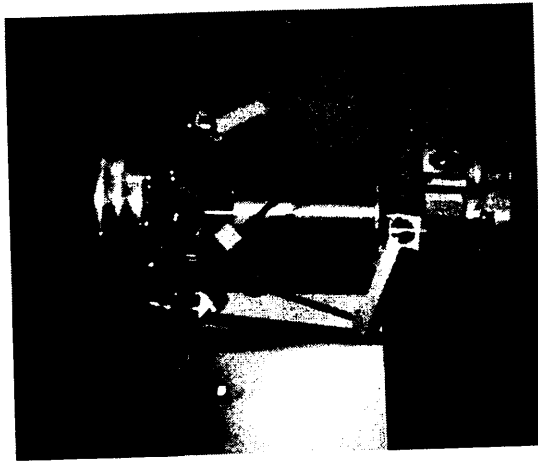


Figure 11. The cybernetic shoulder with $\phi 3\text{mm}$ carbon fiber rod

4.2. Compliance of the cybernetic shoulder

Figure 11 shows the cybernetic shoulder with $\phi 3\text{mm}$ carbon fiber rod link, and we measured the viscosity of the cybernetic shoulder. The configuration of the experimental setup is shown in Figure 12. We measured the oscillation of the end grip when an impulsive disturbance is added. Figure 13 shows the experimental result using $\phi 5\text{mm}$ carbon fiber rod link with damper (dashed line) and without damper (solid line). This figure shows the effectiveness of the damper. In order to evaluate the effect of viscosity on damping, the maximum amplitude of swings are normalized in the figure. Regarding the temper memory alloy, the elasticity and viscosity vary depending on the temperature[8]. By the choice of the phase transformation temperature, we can design the property of links, which is shown in Figure 14 using $\phi 4.31\text{mm}$ SMA links (cool and heated).

5. Conclusions

In this paper, we proposed, designed and fabricated a new shoulder mechanism (the cybernetic shoulder) for humanoid robots. The followings and the

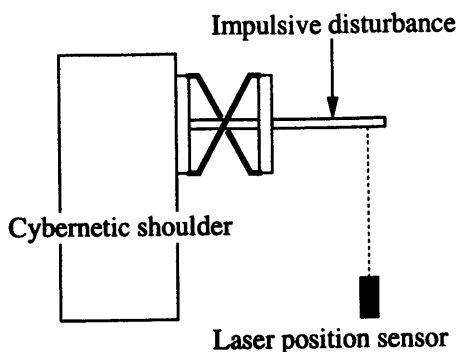


Figure 12. Experimental setup

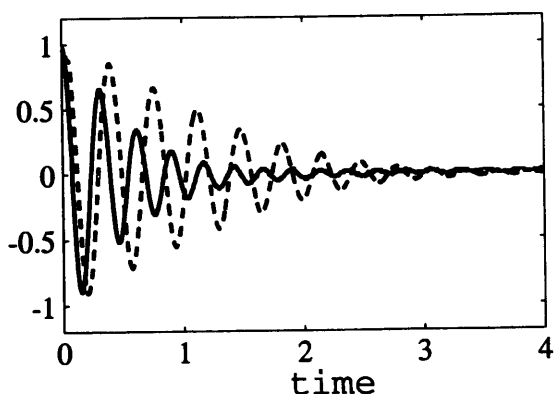


Figure 13. Disturbance responses ($\phi 5\text{mm}$ carbon fiber link with a damper and without damper)

summary of outcomes:

1. The advantages of the cybernetic shoulder are compactness, large and singularity free work space, human-like mobility and small backlash.
2. Taking an advantage of closed kinematic chain structure, the cybernetic shoulder allows mechanical compliance and damping design by appropriate choice of materials.
3. We design the viscosity of link E using temper foam[®] and shape memory alloy.

The authors would like to thank Mr. N. Mizushima for his help with the experimental setup. This research was supported through the Research for the Future Program, the Japan Society for the Promotion of Science (Project No. JSPS-RFTF96P00801).

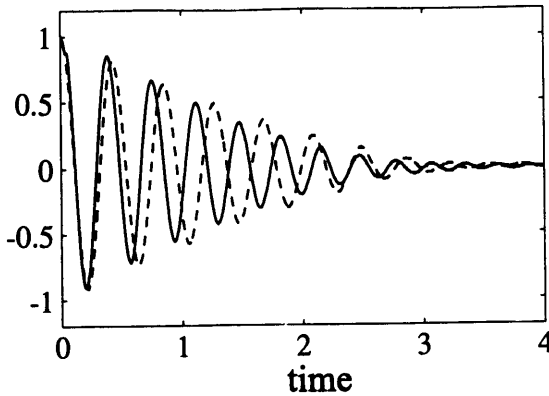


Figure 14. Disturbance responses of link 3(solid line) and heated link 3(dashed line)

References

- [1] J.Yamaguchi and A.Takanishi: Development of a Biped Walking Robot Having Antagonistic Driven Joints Using Nonlinear Spring Mechanism; Proc. of the IEEE International Conference on Robotics and Automation, pp. 185-192 (1997)
- [2] K.Hirai, M.Hirose, Y.Haikawa and T.Takenaka: The Development of Honda Humanoid Robot; Proc. of the IEEE International Conference on Robotics and Automation, pp. 1321-1326 (1997)
- [3] M.E.Rosheim: Robot Evolution, The Development of Anthrobotics; JOHN & SONS, INC., (1994)
- [4] M.Inaba, T.Ninomiya, Y.Hoshino, K.Nagasaka, S.Kagami and H.Inoue: A Remort-Brain Full-Body Humanoid with Multisensor Imaging System of Binocular Viewer, Ears, Wrist Force ant Tactile Sensor Suit; Proc. of the International Conference on Robotics and Automation, pp. 2497-2502 (1997)
- [5] I.A.Kapandji: Physiologie Articulaire; Maloine S.A. Editeur, (1980)
- [6] W. Pollard: Position Controlling Apparatus; U.S. Patent 2,286,571, (1942)
- [7] J.P. Trevelyan: Skills for a Shearing Robot : Dexterity and Sensing; Robotics Research, pp. 273-280 (1985)
- [8] A.Terui, T.Tateishi, H.Miyamoto and Y.Suzuki: Study on Stress Relaxation Properties of NiTi Shape Memory Alloy; Trans. of the Japan Society of Mechanical Engineering (A), Vol.51, No.462,(1985) (in Japanese)